

# Journal of Fluid Mechanics

<http://journals.cambridge.org/FLM>

Additional services for *Journal of Fluid Mechanics*:

Email alerts: [Click here](#)

Subscriptions: [Click here](#)

Commercial reprints: [Click here](#)

Terms of use : [Click here](#)



---

## Resonant-wave signature of an oscillating and translating disturbance in a two-layer density stratified fluid

MOHAMMAD-REZA ALAM, YUMING LIU and DICK K. P. YUE

Journal of Fluid Mechanics / Volume 675 / May 2011, pp 477 - 494  
DOI: 10.1017/S0022112011000309, Published online: 06 April 2011

**Link to this article:** [http://journals.cambridge.org/abstract\\_S0022112011000309](http://journals.cambridge.org/abstract_S0022112011000309)

### How to cite this article:

MOHAMMAD-REZA ALAM, YUMING LIU and DICK K. P. YUE (2011). Resonant-wave signature of an oscillating and translating disturbance in a two-layer density stratified fluid. *Journal of Fluid Mechanics*, 675, pp 477-494 doi:10.1017/S0022112011000309

**Request Permissions :** [Click here](#)

# Resonant-wave signature of an oscillating and translating disturbance in a two-layer density stratified fluid

MOHAMMAD-REZA ALAM,  
YUMING LIU AND DICK K. P. YUE†

Department of Mechanical Engineering, Center for Ocean Engineering,  
Massachusetts Institute of Technology, Cambridge, MA 02139, USA

(Received 8 October 2010; revised 7 January 2011; accepted 13 January 2011;  
first published online 6 April 2011)

We investigate the nonlinear wave signature of a translating and oscillating disturbance under the influence of ambient waves in a two-layer fluid. The main interests are the generation and features of the far-field waves due to nonlinear wave resonances. We show, using perturbation theory, that free waves on the surface and/or interface can be produced by triad-resonant interactions, a mechanism not obtained in a homogeneous fluid. These occur among the radiated waves due to the disturbance motion (disturbance waves); and between the disturbance waves and free ocean waves (ambient waves). Such resonance-generated waves can appear upstream or downstream, and may propagate away from or towards the disturbance. In realistic situations where ambient waves and disturbance oscillations contain multiple frequencies, numerous resonant and near-resonant interactions at second and higher orders may occur, making the theoretical analysis of the problem intractable. For this purpose, we develop a direct simulation capability using a high-order spectral method, which provides independent validation of the theoretical predictions. Our investigations show that, under specific but realistic conditions, resonance interactions may lead to significant far-field short waves that are more amenable to remote sensing. If the characteristics of the disturbance are known, we illustrate how nonlinear wave resonances provide a mechanism for more precise estimation of ocean stratification properties using surface wave measurements. Finally we show that when a moving disturbance oscillates at multiple frequencies, ensuing multiple resonances may lead to energy spreading across a broader spectrum, resulting in the loss of information about the body motion.

**Key words:** interfacial flows (free surface), surface gravity waves

---

## 1. Introduction

We address the problem of nonlinear interactions among surface and interfacial waves of a translating and oscillatory disturbance with and without the participation of an ambient wave in a two-layer (density stratified) fluid. The focus is on the understanding of the mechanism and characteristics of wave generation via second-order resonant-wave interactions in a multi-layer fluid. The study is motivated by

† Email address for correspondence: yue@mit.edu

the potential use of surface measurements for determination and identification of the traces of ships or submarines in strong two-layer waters such as littoral zones of warm seas and oceans.

There are numerous studies on the wave signatures associated with moving object in a homogeneous fluid. When a body travels (steadily) forward in calm water, a so-called Kelvin wave pattern behind the body is known to be formed (e.g. Debnath 1994). The effect of nonlinearities on the wave pattern has also been investigated (Newman 1971; Akylas 1987). When ambient waves are present, the body inevitably undergoes oscillations. In addition to the steady Kelvin waves associated with the steady forward motion, distinctive unsteady waves are radiated by the oscillatory motion. Depending on the frequency of the body oscillation and the forward speed of the body, the radiated waves may appear far upstream and/or downstream of the body. There exist limited studies on the effect of nonlinearities on the unsteady wave pattern. Among these, it is known that resonant interactions among the steady and unsteady waves (generated by the body motion) cannot occur (D'yachenko & Zakharov 1994). When the interaction with the ambient waves is considered, a third-order resonant quartet can be formed between the steady Kelvin waves and the unsteady ambient wave, leading to the generation of a new propagating wave along a specific ray in the Kelvin wake (Zhu, Liu & Yue 2008).

Many open seas, oceans and lakes are, however, stratified. In addition to surface waves, internal waves also exist in a density-stratified fluid (see e.g. Garrett & Munk 1979; Kunze *et al.* 2002). In many shallow seas and oceans, the fluid densities above and below the thermocline are nearly constant. Therefore, the thermocline can be approximated by a plane of a sudden density change that admits propagating waves. This is called a two-layer approximation of density stratified fluids. The waves propagating over the plane of the sudden density change are called as interfacial waves. In a two-layer fluid, the number of propagating waves generated by a two-dimensional translating and oscillating disturbance doubles compared to that in a homogeneous fluid (Alam, Liu & Yue 2009a). When nonlinear wave interactions are considered, the interfacial waves must also be accounted for. As a result, unlike in a homogeneous fluid, a triad-resonant interaction between surface and interfacial waves is known to occur in a two-layer fluid (Ball 1964; Wen 1995; Hill & Foda 1996). It remains of interest to know whether the resonant interactions among the ship waves themselves or between the ship waves and ambient waves can occur in a two-layer stratified fluid. This is the objective of this work.

In this study, by analysing the basic characteristics of the waves in the wake of a two-dimensional translating and oscillating (ship) disturbance in a two-layer fluid, we show that under certain specific (yet realistic) conditions a pair of disturbance waves can form a triad resonance to generate a new free wave that normally travels away from the disturbance. In addition, a similar triad resonance can occur between the distance wave and an ambient wave (that has the same frequency as the disturbance oscillation). The resonance-generated wave can travel towards the disturbance. These nonlinear resonant interactions can produce distinctive wave patterns in the wake of the moving disturbance, which may have significant implications in the inverse problem of detecting the presence of the submerged objects (Wren & May 1997) or estimating the ocean physical properties by the surface measurements (Avital & Miloh 1994, 1999).

We first present the mathematic formation of the general nonlinear problem and outline the basic characteristics of the linear wave system generated by a translating and oscillating disturbance in a two-layer fluid (§ 2). When the second-order

nonlinearity is taken into account, triad-resonant wave–wave interaction can occur under the certain resonance condition (§ 3.1). Two classes of triad resonances exist with and without the participation of the ambient wave in the interactions. To understand the basic characteristics of the triad resonance, the amplitude evolution equations for interacting waves are derived via a multiple scale analysis, from which some distinctive features for the resonance-generated wave under various conditions can be deduced (§§ 3.2 and 3.3). Realistic ocean waves, however, are often composed of multiple wave components with different frequencies. As a result, a number of resonant and near-resonant interactions may happen simultaneously. To address the practical situations, an effective direct simulation capability is developed based on the extension of a high-order spectral (HOS) method to a two-layer fluid with the presence of an oscillating and translating disturbance (§ 4). The numerical simulations are validated by comparisons with the perturbation theory prediction in relatively simple cases (§ 5.1). The simulations are then used to elucidate the distinctive characteristics of the surface and interface associated with the triad-resonant wave–wave interactions, which can be used, via surface measurements, in the characterization of underwater objects (§ 5.2) and in the inverse problem for the estimate of fluid stratification properties (§ 5.3). To understand the effect of the resonant-wave interactions in realistic ocean environment, we consider an illustrative example in which the disturbance oscillates with three different frequencies. Multiple-resonant and near-resonant interactions among the disturbance waves occur. As a result, a wide-spreading wave spectrum in the wake of the disturbance is obtained (§ 5.4). The conclusions are drawn in § 6.

## 2. Problem formulation

We consider the problem of nonlinear wave generation by a two-dimensional oscillating and travelling disturbance in a two-layer fluid. The upper and lower fluid layers have respectively mean depths  $h_u$  and  $h_\ell$ , and fluid densities  $\rho_u$  and  $\rho_\ell$  (subscripts  $u$  and  $\ell$  hereafter denote quantities associated with the upper and lower fluid layers, respectively). A Cartesian coordinate system  $(x, z)$  is defined with the  $x$ -axis on the mean free surface and the  $z$ -axis positive upward. The two-layer fluid rests on a flat horizontal bottom  $z = -h_u - h_\ell$ . Without loss of generality, the disturbance is modelled as a point source that is initially located at  $x = x_0$  and travels in the upper layer at a fixed depth  $z = z_0$  with a forward velocity  $u = U\hat{i}$ , where  $\hat{i}$  is the unit vector in the positive  $x$ -direction and  $U$  is the magnitude of the velocity. A plane ambient wave with frequency  $\omega_a$  and wavenumber  $k_a$  is assumed to be present on the ocean surface and propagate in the  $x$ -direction. In response to the action of the ambient wave, the disturbance normally oscillates at the encounter frequency  $\omega_0 = \omega_a - Uk_a$ . To model the oscillation of the disturbance, for simplicity, we let the point source to have an oscillatory strength  $m \cos \omega_0 t$  while keeping its depth constant. Throughout this paper, we assume that the ambient wave exists on the surface and the disturbance oscillates with a given (constant) amplitude at the encounter frequency of the ambient wave.

We assume that the fluids in both layers are homogeneous, incompressible, immiscible and inviscid so that the fluid motion in each layer is irrotational. The effect of surface tension is neglected. The flow in each layer is described by a velocity potential,  $\phi_u(x, z, t)$  and  $\phi_\ell(x, z, t)$ . The nonlinear governing equations are

$$\nabla^2 \phi_u = m \delta(x - x_0 - Ut, z - z_0) \cos \omega_0 t \quad -h_u + \eta_i < z < \eta_s \quad (2.1a)$$

$$\nabla^2 \phi_\ell = 0 \quad -h_u - h_\ell < z < -h_u + \eta_i \quad (2.1b)$$

$$\eta_{s,t} + \eta_{s,x} \phi_{u,x} - \phi_{u,z} = 0 \quad z = \eta_s \quad (2.1c)$$

$$\phi_{u,t} + \frac{1}{2}(\phi_{u,x}^2 + \phi_{u,z}^2) + g\eta_s = 0 \quad z = \eta_s \quad (2.1d)$$

$$\eta_{i,t} + \eta_{i,x}\phi_{u,x} - \phi_{u,z} = 0 \quad z = -h_u + \eta_i \quad (2.1e)$$

$$\eta_{i,t} + \eta_{i,x}\phi_{\ell,x} - \phi_{\ell,z} = 0 \quad z = -h_u + \eta_i \quad (2.1f)$$

$$\rho_u [\phi_{u,t} + \frac{1}{2}(\phi_{u,x}^2 + \phi_{u,z}^2) + g\eta_i] - \rho_\ell [\phi_{\ell,t} + \frac{1}{2}(\phi_{\ell,x}^2 + \phi_{\ell,z}^2) + g\eta_i] = 0 \quad z = -h_u + \eta_i \quad (2.1g)$$

$$\phi_{\ell,z} = 0 \quad z = -h_u - h_i, \quad (2.1h)$$

where  $\eta_s(x, t)$  and  $\eta_i(x, t)$  are the elevations of the free surface and the interface respectively,  $g$  is the gravity acceleration and  $\delta$  is the Dirac delta function. Equations (2.1a) and (2.1b) are the continuity equations. Equations (2.1c) and (2.1d) are respectively the kinematic and dynamic boundary conditions on the free surface, which are identical to those in a homogenous fluid. Equations (2.1e) and (2.1f) represent the kinematic boundary condition on the interface, ensuring the immiscibility of the two-layer fluid. Equation (2.1g) is the dynamic boundary condition on the interface, which guarantees the continuity of the pressure on the interface. Equation (2.1h) is the classical kinematic condition on the stationary impermeable bottom. If the source is located in the lower layer, the right-hand sides of (2.1a) and (2.1b) need to be exchanged, but the rest of the discussion in this section remains the same.

For a (linear) freely propagating wave with frequency  $\omega$  and wavenumber  $k$  in a two-layer fluid (in a space-fixed coordinate system), the dispersion relation is well known (Lamb 1932):

$$\mathcal{D}(\omega, k) \equiv \omega^4(\mathcal{R} + \coth kh_u \coth kh_\ell) - \omega^2 gk(\coth kh_u + \coth kh_\ell) + g^2 k^2(1 - \mathcal{R}) = 0, \quad (2.2)$$

where  $\mathcal{R} \equiv \rho_u/\rho_\ell$  is the density ratio. For a given  $k > 0$ , in general, (2.2) has four roots:  $\pm\omega_s(k)$ ,  $\pm\omega_i(k)$ , with  $\omega_s > \omega_i > 0$  (Ball 1964), where  $\pm\omega_s$  and  $\pm\omega_i$  denote the frequencies of the surface-mode and interfacial-mode waves respectively (Alam, Liu & Yue 2009b).

If we consider the linearized form of (2.1), only a finite number of propagating waves can exist in the far field of the disturbance (Alam *et al.* 2009a). The wavenumber and frequency of each such wave must satisfy the dispersion relation (2.2). In a frame of reference moving with the disturbance, the wavenumbers ( $k_n$ ) of these waves are given by the real solutions of (2.2) with  $\omega$  replaced by  $\pm\omega_0 + Uk_n$  (see e.g. Faltinsen 1993), that is,

$$\mathcal{D}(\pm\omega_0 + Uk_n, k_n) = 0. \quad (2.3)$$

For a specified  $\omega_0$ , there are always four real solutions for  $k_n$  corresponding to the case with the plus sign in (2.3). For the case with the minus sign in (2.3), the number of real solutions for  $k_n$  however reduces from 4 to 2 and then to 0 as  $U$  increases (starting from 0). As a result, (2.3) may have a total of  $N_w = 8, 6$  or 4 real ( $k_n$ ) solutions for a given  $\omega_0$ , depending on the density ratio  $\mathcal{R}$ , the dimensionless frequency  $\tau \equiv U\omega_0/g$ , the depth ratio  $h \equiv h_u/H$ , where  $H = h_u + h_\ell$ , and the Froude number  $\mathcal{F} \equiv U^2/(gH)$ . For  $N_w = 8$ , half of them are surface-mode waves ( $n = 1, 2, 3$  and 4) and the other half are interfacial-mode waves ( $n = 5, 6, 7$  and 8). With  $C_{g,n}$  denoting the group velocity of the wave with wavenumber  $k_n$  (in the space-fixed coordinate system), we number these waves with the property:  $C_{g,2} > U$ ,  $C_{g,4} < 0$ ;  $C_{g,6} > U$ ,  $C_{g,8} < 0$ ;  $0 < C_{g,3} < C_{g,1} < U$  and  $0 < C_{g,7} < C_{g,5} < U$  (see also Alam *et al.* 2009a). Clearly, waves  $k_2$  and  $k_6$  propagate ahead, while waves  $k_1, k_3, k_4, k_5, k_7$  and

$k_8$  propagate behind the disturbance. We note that when  $N_w = 6$ , we have all four surface waves but only two interfacial waves ( $n = 7$  and  $8$ ). When  $N_w = 4$ , we have two surface waves ( $n = 3$  and  $4$ ) and two interfacial waves ( $n = 7$  and  $8$ ).

### 3. Triad resonant interactions

#### 3.1. Resonance condition

Based on the linear analysis,  $N_w$  far-field waves of a two-dimensional (2D) oscillating and translating disturbance propagate indefinitely without any change in their amplitudes. We show here that if nonlinearity is taken into account a pair of these waves can resonate to generate a new free wave via a triad wave–wave resonance mechanism. This obtains under specific but realizable conditions. The phenomenon is important because the generation of new free waves leads to changes in the wave signature and spectrum on both the surface and interface (e.g. § 5.4), which are not obtained in the context of linear theory nor if stratification is overlooked.

If two waves, say with the wavenumber and frequency  $(k', \omega')$  and  $(k'', \omega'')$  respectively, satisfy the condition  $\mathcal{D}(\omega_r, k_r) = 0$ , where  $k_r = k' \pm k''$  and  $\omega_r = \omega' \pm \omega''$ , then waves  $k', k''$  and  $k_r$  are in resonance and energy can flow from waves  $(k', k'')$  into the resonant wave  $(k_r)$ . Although triad resonances of gravity waves are known to be degenerate in a homogeneous fluid (D'yachenko & Zakharov 1994), in a two-layer fluid Ball (1964) showed that two counter-propagating surface waves can resonate an interfacial wave. Later Wen (1995) further showed that two counter-propagating interfacial waves can form a triad resonance with a free-surface wave. To determine if the resonance condition is satisfied between  $N_w$  disturbance waves, for given ocean and disturbance parameters  $h, \mathcal{R}, \tau$  and  $\mathcal{F}$ , the resonance condition needs to be examined for all pairs of waves that both exist on the same (upstream or downstream) side of the disturbance. (Note that since the disturbance waves propagate away from the disturbance, an upstream disturbance wave cannot interact with a downstream wave.)

In practice, the oscillation of the disturbance can be forced artificially or obtained in response to the action of ambient ocean waves. In this paper, we always assume that the ambient wave exists on the surface and the disturbance oscillation frequency is equal to the encounter frequency of the ambient wave. The ambient wave, however, may or may not directly participate in the resonant interaction. To understand all possible scenarios of such resonances, we consider an ambient wave with wavenumber  $k_a$  and frequency  $\omega_a$ . The oscillation frequency of the disturbance  $\omega_0$  is related to  $\omega_a$  by the relation  $\omega_0 = \omega_a \pm Uk_a$ , where  $\pm$  corresponds to the head ( $UC_{g,a} < 0$ ) and following sea ( $UC_{g,a} > 0$ ) condition respectively. The wavenumber  $k_a$  is identical to the wavenumber of any one of  $N_w$  far-field waves of the disturbance. For example, and without loss of generality, if we let  $k_a = k_2$  then the wave  $k_2$  is seen on both sides of the disturbance. For clarity, we classify all resonance cases as class I, in which the ambient wave does not participate in the resonance, and class II, in which the ambient wave participates in the resonance. Note that in class I, resonance is formed merely between the disturbance waves. Therefore, it appears even if the disturbance is artificially forced to oscillate without the presence of an ambient wave.

Under the deep-layer assumption ( $k_n h_u, k_n h_\ell \gg 1$ ,  $n = 1, \dots, 8$ ), simple closed-form solutions for the wavenumbers of the interacting waves that can form a resonant triad for given  $\mathcal{F}, h, \tau$  and  $\mathcal{R}$  can be obtained. However, as is expected, in this case the resonance is weak and has a little practical relevance. In a finite-depth water, the solutions have to be sought numerically from the general resonance condition for a wide range of parameters  $\mathcal{F}, h, \tau$  and  $\mathcal{R}$ . Table 1 lists all resonance cases as  $\tau$  varies

Case no.	$\tau$	$m$	$n$	$\omega_r/\omega_0$	$I/S$	Case no.	$\tau$	$m$	$n$	$\omega_r/\omega_0$	$I/S$
$a_1$	0.0522	1	-3	2.0111	$I$	$b_1$	0.2747	4	7	0.32059	$I$
$a_2$	0.0699	1	-7	11.902	$S$	$b_2$	1.234	4	-7	0.72906	$S$
$a_3$	0.0894	2	8	0.58833	$I$	$b_3$	2.821	4	-8	0.3189	$S$
$a_4$	0.0900	1	7	11.111	$S$	$b_4$	3.886	7	-8	0.23132	$S$
$a_5$	0.1235	3	-7	8.0973	$S$	$b_5$	9.004	3	4	0.11108	$I$
$a_6$	0.1236	4	-8	0.42525	$I$	Case no.	$\tau$	$m$	$n$	$\omega_r/\omega_0$	$I/S$
$a_7$	0.1302	2	-8	1.6469	$S$	$c_1$	9.075	3	4	0.11054	$I$
$a_8$	0.1516	2	4	0.34708	$I$						
$a_9$	0.1843	2	-7	0.62626	$I$						
$a_{10}$	0.1873	3	7	6.8890	$S$						
$a_{11}$	0.2493	1	-2	0.21225	$I$						
$a_{12}$	0.2499	1	-7	1.4647	$S$						
$a_{13}$	0.6557	4	7	0.36258	$I$						
$a_{14}$	1.233	4	-7	0.81130	$S$						
$a_{15}$	3.337	4	-8	0.29975	$S$						
$a_{16}$	4.738	7	-8	0.21108	$S$						
$a_{17}$	9.004	3	4	0.11108	$I$						

TABLE 1. Cases of triad resonance in a finite-depth two-layer fluid for  $\mathcal{R}=0.9$ ,  $h=0.33$ , and  $\mathcal{F}=0.005$  (left table, case numbers  $a_k$ );  $\mathcal{F}=0.60$  (right top table, case numbers  $b_k$ );  $\mathcal{F}=2$  (right bottom table, case numbers  $c_k$ ). At each given  $\tau$ , waves  $k_m$  and  $k_n$  form a triad resonance that generates an interfacial or surface-mode wave (denoted by  $I/S$ ) with frequency  $\omega_r$  (normalized by  $\omega_0$ ).

for fixed  $\mathcal{R}$  and  $h$  with three different  $\mathcal{F}$  values. The numbered symbols  $a_k$ ,  $b_k$  and  $c_k$  denote the resonance cases associated with  $\mathcal{F}=0.005$ ,  $0.6$  and  $2$  respectively. Each case corresponds to a specific  $\tau$  under which the resonance condition is satisfied by the two waves with wavenumbers  $k_m$  and  $\pm k_n$ , and a third wave with wavenumber  $k_r \equiv k_m \pm k_n$  and frequency  $\omega_r$  (normalized by  $\omega_0$ ) that is generated by the resonance. From the dispersion relation satisfied by  $k_r$  and  $\omega_r$ , we can determine whether the resonant wave is a surface or interfacial wave ( $I/S$ ). For example, case  $a_{11}$  states that at  $\tau=0.2493$  ( $\mathcal{F}=0.005$ ,  $h=0.33$  and  $\mathcal{R}=0.9$ ), waves  $k_1$  and  $k_2$  can have a resonant interaction to generate a free interfacial wave ( $I$ ) with  $k_r=k_1-k_2$  and  $\omega_r/\omega_0=0.2123$ .

Clearly, as  $\mathcal{F}$  increases the number of resonance cases decreases. This is due to the fact that as  $\mathcal{F}$  increases the number of disturbance waves ( $N_w$ ) decreases. Note that in table 1, cases  $a_3$ ,  $a_7$ ,  $a_8$ ,  $a_9$  and  $a_{11}$  are class I resonance, and the rest are class II resonance. In the following, we study the properties of classes I and II resonances in more details.

### 3.2. Class I resonance

In class I triad resonance, two disturbance waves interact resonantly to generate a free wave. In principle, this class of resonant triads can be formed ahead of the disturbance such as  $(k_2, k_6$  and  $k_r)$  (no such a case is seen for the parameters considered in table 1) and/or behind the disturbance like  $(k_n, k_m, k_r)$ ,  $m, n \in \{1, 3, 4, 5, 7, 8\}$ ,  $m \neq n$  (all except  $a_3, a_7, a_8, a_9$  and  $a_{11}$  in table 1 belong to this group). Let the relative group speed of the resonant wave (in the coordinate system moving with the disturbance) to be  $C_{g,r}^{(d)} = -U + C_{g,r}$ , where  $C_{g,r}$  is the group speed of the resonant wave in the space fixed coordinate system. It can be easily shown that  $C_{g,r}^{(d)} > 0$  (or  $< 0$ ) for class I triads formed at upstream (or downstream) of the disturbance. This indicates that all the

waves generated by class I resonances propagate away from the disturbance whether they are located at upstream or downstream.

In a resonance triad, the interacting waves exchange their energy with each other. The evolution equations governing the amplitudes of these waves can be derived by a standard multiple-scale analysis (cf. Craik 1988) or equivalently by an energy argument. Away from the near field of the disturbance and in the moving coordinate system, the system of evolution equations takes the form

$$\frac{\partial A_1}{\partial t} + C_{g,1}^{(d)} \frac{\partial A_1}{\partial x} = \beta_1 A_2 A_r, \quad \frac{\partial A_2}{\partial t} + C_{g,2}^{(d)} \frac{\partial A_2}{\partial x} = \beta_2 A_1 A_r, \quad \frac{\partial A_r}{\partial t} + C_{g,r}^{(d)} \frac{\partial A_r}{\partial x} = \beta_r A_1 A_2, \quad (3.1)$$

where  $A_1$  and  $A_2$  are the (complex) amplitudes of the two disturbance waves and  $A_r$  is the (complex) amplitude of the resonance-generated wave. In the above equations, coefficients  $\beta_1$ ,  $\beta_2$  and  $\beta_r$  are the constants and functions of the physical parameters of the problem. These coefficients are algebraically lengthy and are given, e.g. by Alam (2008). Neglecting the near-field waves, we set the initial and boundary conditions as

$$A_1(x, 0) = 0, \quad A_1(0, t) = A_{10}, \quad A_2(x, 0) = 0, \quad A_2(0, t) = A_{20}, \quad A_r(x, 0) = 0, \quad (3.2)$$

where  $A_{10}$  and  $A_{20}$  are the far-field amplitudes of the two disturbance waves participating in the resonance (Alam *et al.* 2009a). Equation (3.1) has a steady-state solution that can be expressed in a closed form in terms of Jacobian elliptic functions (Ball 1964). In this solution, all wave amplitudes oscillate slowly with the distance from the disturbance. Near the disturbance where the resonance first starts, the amplitude of the resonant wave grows linearly with the interaction distance  $|x^{(d)}|$ :

$$A_r(x) = \frac{\beta_r |x^{(d)}|}{C_{g,r}^{(d)}}. \quad (3.3)$$

Clearly,  $A_r$  becomes unbounded if  $C_{g,r}^{(d)} \rightarrow 0$ . This is similar to the linear solution of the unsteady disturbance oscillation problem near the critical speed. In this situation, higher order nonlinearities are important and need to be taken into account (see for example Dagan & Miloh 1982; Akylas 1984; Liu & Yue 1993, for the treatment of near critical speeds in homogeneous fluids).

### 3.3. Class II resonance

In class II triad resonance, the ambient wave participates in the interaction. This class of resonances can be further categorized into two groups.

#### 3.3.1. Group a. Resonant wave moves away from the disturbance

In this group, except for the participation of the ambient wave ( $k_a$ ) in the resonance, the behaviour of the resonant wave is similar to that in class I in the sense that it travels away from the disturbance. This group of triad resonances can be formed in upstream by waves ( $k_a, k_n, k_r$ ), where  $n = 2$  and  $6$  and  $k_a = k_p$ ,  $p = 1, 3, 4, 5, 7$  and  $8$  (i.e. in a head sea), with  $C_{g,r}^{(d)} > 0$  (no such a case is shown in table 1), or in downstream by waves ( $k_a, k_m, k_r$ ), where  $m = 1, 3, 4, 5, 7$  and  $8$  and  $k_a = k_q$ ,  $q = 2$  and  $6$  (i.e. in a following sea), with  $C_{g,r}^{(d)} < 0$  (cases  $a_3, a_7, a_8, a_9$  and  $a_{11}$  in table 1). The variation of the amplitudes of the interacting waves behaves similarly to that in class I resonance.

### 3.3.2. Group b. Resonant wave moves toward the disturbance

In this group, as in group a, the ambient wave ( $k_a$ ) participates in the resonance. However, the resonance-generated wave ahead/behind the disturbance moves backward/forward (i.e. towards) the disturbance and eventually encounters the disturbance. This group of second-order resonant triads can be formed at upstream by waves ( $k_a, k_n, k_r$ ), where  $n=2$  and  $6$  and  $k_a=k_p$ ,  $p=1, 3, 4, 5, 7$  and  $8$  (i.e. in a head sea), with  $C_{g,r}^{(d)} < 0$  (cases  $a_3, a_7, a_8, a_9$  and  $a_{11}$  in table 1). They can also be formed at downstream by waves ( $k_a, k_m, k_r$ ), where  $m=1, 3, 4, 5, 7$  and  $8$  and  $k_a=k_q$ ,  $q=2$  and  $6$  (i.e. in a following sea), with  $C_{g,r}^{(d)} > 0$  (no such a case in table 1). This is an important case since the resonant wave, upon passing over the disturbance, can force the disturbance to oscillate at the frequency  $\omega_r$ , different than  $\omega_0$ . Due to this oscillation, the disturbance generates a new group of waves that make the wake pattern more complex, and new resonances may emerge.

The evolution of the amplitudes of the interacting waves in group-b resonances is much more complicated than in group-a resonances. Since the resonance-generated wave travels towards the disturbance from the far field, evolution of the resonant-wave envelope does not reach a steady state. Furthermore, after the resonant wave passes over the disturbance, this group of resonance continues to the other side of the disturbance where the disturbance wave component in the triad can be generated by the resonance. (Note that this component of the disturbance wave does not exist on this side of the disturbance in the steady linear solution.) The generated wave again moves towards the disturbance. It can pass over the disturbance to the other side and participate in the (original) resonance there. To find the evolution of the interacting waves in this type of resonances, the initial boundary-value problem (2.1) needs to be fully solved.

As an example, we consider case  $a_3$  of table 1, where the resonance triad is formed by waves ( $k_a=k_8, k_2, k_r$ ). From analysing the dispersion relation it can be shown that the oscillation of the disturbance, which moves in the positive  $x$ -axis in the head sea with  $k_a=k_8$  ( $C_{g,8}^{(d)} < 0$ ), generates six free waves including  $k_2$  ( $C_{g,2}^{(d)} > 0$ ). Waves  $k_2$  and  $k_8$  interact resonantly ahead of the disturbance to generate a (new) wave  $k_r$  that has a negative relative group speed ( $C_{g,r}^{(d)} < 0$ ). Wave  $k_r$  moves toward the disturbance and acts as a new head-sea ambient wave. A part of the energy of this resonant wave is used to excite the oscillation of the disturbance and the rest keeps moving along the  $-x$  axis. Since the ambient waves  $k_a=k_8$  already exist at  $x^{(d)} < 0$ , once wave  $k_r$  passes over the disturbance, they continue the resonant interaction to generate wave  $k_2$  (previously only exists at  $x^{(d)} > 0$ ) at  $x^{(d)} < 0$ . The generated wave  $k_2$  moves towards the disturbance as  $C_{g,2}^{(d)} > 0$ . The cascade of such multiple-resonant interactions, in principle, goes on indefinitely at both sides of the disturbance.

We note that group-b resonance, with the resonant wave moving towards the disturbance, may also occur without the participation of the ambient wave (i.e. in class I resonance), but can occur only for very strong stratifications that may not be obtained in the real ocean. As an example, we can show under deep layer assumptions that for  $\mathcal{R}=0.5$  and  $\tau=0.122$ , the resonant interaction between waves  $k_1$  and  $k_7$  behind the disturbance generates a wave with a positive group velocity larger than  $U$ .

## 4. Direct numerical simulation

In practice, a broadband spectrum of waves exists on the surface and interface of a two-layer ocean. As a result, the disturbance oscillates with multiple frequencies.

A number of triad-resonant or near-resonant interactions may occur simultaneously, making the evolution of the surface/interface waves analytically intractable. We emphasize that although exact resonance conditions are selective, countless near resonances are possible and play an important role in nonlinear wavefield evolution (see e.g. Hammack & Henderson 1993; Staquet & Sommeria 2002; Alam *et al.* 2009b).

Here we present a direct simulation scheme, based on the pseudospectral method, which includes the presence of a moving and oscillating disturbance and the effect of surface/interface nonlinearities. The algorithm is an extension of a HOS method that is originally developed for nonlinear gravity waves in a homogeneous fluid and later extended to a two-layer fluid (Dommermuth & Yue 1987; Alam *et al.* 2009a,b). We here further extend this method for nonlinear wave-wave interactions in the presence of an oscillating and translating disturbance (or body). The developed algorithm preserves the key characteristics of the original HOS method. In particular, it follows the evolution of a large number of surface and interface wave modes (with  $N = O(10^{3\sim 4})$  per dimension) and accounts for their interactions up to an arbitrary high order (with  $M$  up to  $O(10)$  in practice). For moderately steep surface and interface waves, it obtains an exponential convergence of the solution with respect to both  $N$  and  $M$ . The required numerical effort is approximately linear with  $N$  and  $M$ . Extensive convergence tests of the algorithm for a two-layer fluid can be found in Alam (2008).

For completeness, the key formulation of the extended algorithm is outlined here. We define  $\phi_u \equiv \varphi_u + \tilde{\phi}_u$  and  $\phi_\ell \equiv \varphi_\ell + \tilde{\phi}_\ell$ , where  $\tilde{\phi}_{u,\ell}$  represents the simple effects of free stream and Rankine point source and  $\varphi_{u,\ell}$  is the wave perturbation. Following Zakharov (1968), we define the surface potential  $\varphi_u^S$  for the upper layer and the interface potentials  $\varphi_{u/\ell}^S$  for both upper and lower layers by

$$\varphi_u^S(x, t) \equiv \varphi_u(x, \eta_s(x, t), t) \quad \text{and} \quad \varphi_{u/\ell}^I(x, t) \equiv \varphi_{u/\ell}(x, -h_u + \eta_i(x, t), t). \quad (4.1)$$

In the neighbourhood of the interface, for convenience, we define a new potential  $\psi(x, z, t) \equiv \varphi_\ell(x, z, t) - \mathcal{R}\varphi_u(x, z, t)$ . We further define  $\psi^I$  to be the value of  $\psi$  evaluated on the interface. In terms of these quantities, we can rewrite the kinematic and dynamic boundary conditions on the surface ((2.1c) and (2.1d)) and interface ((2.1e) and (2.1g)) in the forms

$$\eta_{s,t} + \eta_{s,x}\varphi_{u,x}^S - (1 + \eta_{s,x}^2)\varphi_{u,z} = \tilde{\phi}_{u,z} - \eta_{s,x}\tilde{\phi}_{u,x}, \quad z = \eta_s, \quad (4.2)$$

$$\begin{aligned} \varphi_{u,t}^S + g\eta_s + 1/2\varphi_{u,x}^{S^2} - 1/2(1 + \eta_{s,x}^2)\varphi_{u,z}^2 \\ = -\tilde{\phi}_{u,x}\varphi_{u,x}^S - 1/2(\tilde{\phi}_{u,x}^2 + \tilde{\phi}_{u,z}^2) - \tilde{\phi}_{u,t}, \quad z = \eta_s, \end{aligned} \quad (4.3)$$

$$\eta_{i,t} + \eta_{i,x}\varphi_{u,x}^I - (1 + \eta_{i,x}^2)\varphi_{u,z} = \tilde{\phi}_{u,z} - \eta_{i,x}\tilde{\phi}_{u,x}, \quad z = -h_u + \eta_i, \quad (4.4)$$

$$\begin{aligned} \psi_{,t}^I + g\eta_i(1 - \mathcal{R}) + 1/2[\varphi_{\ell,x}^{I^2} - \mathcal{R}\varphi_{u,x}^{I^2}] - 1/2(1 + \eta_{i,x}^2)(\varphi_{\ell,z}^2 - \mathcal{R}\varphi_{u,z}^2) \\ = -(\tilde{\phi}_{\ell,x}\varphi_{\ell,x}^I - \mathcal{R}\tilde{\phi}_{u,x}\varphi_{u,x}^I) - 1/2[(\tilde{\phi}_{\ell,x}^2 + \tilde{\phi}_{\ell,z}^2) - \mathcal{R}(\tilde{\phi}_{u,x}^2 + \tilde{\phi}_{u,z}^2)] \\ - (\tilde{\phi}_{\ell,t} - \mathcal{R}\tilde{\phi}_{u,t}), \quad z = -h_u + \eta_i. \end{aligned} \quad (4.5)$$

In the time simulation of nonlinear two-layer fluid motion with the HOS approach, (4.2)–(4.5) are used as the evolution equations for  $\eta_s$ ,  $\varphi_u^S$ ,  $\eta_i$  and  $\psi^I$  provided that the vertical surface velocity,  $\varphi_{u,z}(x, \eta_s, t)$ , and the vertical interface velocities,  $\varphi_{u,z}(x, -h_u + \eta_i, t)$  and  $\varphi_{\ell,z}(x, -h_u + \eta_i, t)$ , are obtained from the boundary-value solution with a desired order  $M$  (Alam *et al.* 2009b). In the present problem with the oscillating source located in the upper layer, we have  $\tilde{\phi}_u = Ux + m_0/2\pi(\ln r_1 + \ln r_2) \sin \omega_0 t$  and

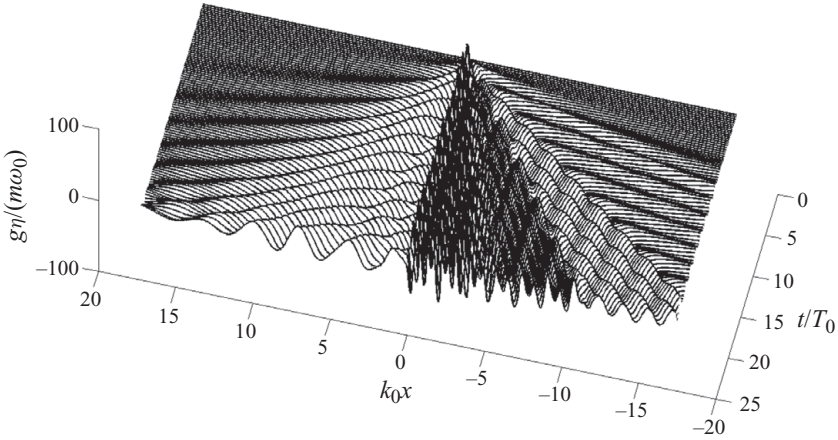


FIGURE 1. Water-fall plot of time evolution of the interfacial waves, in the moving frame of reference, due to an oscillating and translating disturbance in a two-layer fluid. Physical parameters are  $\mathcal{R} = 0.9$ ,  $\tau = 0.2$ ,  $\mathcal{F} = 0.004$ ,  $h = 0.005$ ,  $z_0/h_u = 0.5$ , and the dimensionless source strength  $m/(\omega_0 H^2) = 5.1e^{-6}$ . Numerical parameters are  $N = 4096$ ,  $N_t = 64$ ,  $M = 3$ , and  $L = 32\lambda_4$ . Only a portion of the computational domain is shown ( $T_0 = 2\pi/\omega_0$ ).

$\tilde{\phi}_\ell = Ux$ , where

$$r_1^2 = \sin^2\left(\frac{x - x_0}{2L/\pi}\right) + \sinh^2\left(\frac{z - z_0}{2L/\pi}\right), \quad r_2^2 = \sin^2\left(\frac{x - x_0}{2L/\pi}\right) + \sinh^2\left(\frac{z + 2h_u + z_0}{2L/\pi}\right), \tag{4.6}$$

with  $L$  being the length of the (periodic) computational domain. Similar expressions can be derived for the source located in the lower layer. For the numerical results presented, parameters such as nonlinearity order  $M$ , number of spectral modes  $N$  and time step  $N_t = T/\Delta t$ , where  $T$  is the period of the shortest wave in the wavefield, are specified. For the numerical results we present later, typically  $N = O(10^3)$  and  $M = 3$  or 4, which are sufficient for the study of second-order triad-resonant wave-wave interactions of interest.

Figure 1 shows a sample result of the time evolution of the waves on the interface generated by an oscillating and translating disturbance ( $\tau = 0.2$ ,  $\mathcal{F} = 0.004$ ) in a two-layer fluid ( $\mathcal{R} = 0.9$ ,  $h = 0.005$ ). The disturbance, initially located at  $x = 0$  and  $z_0 = 0.5h_u$ , starts to oscillate and translate in the positive  $x$ -direction at  $t = 0$ . For these parameters, a total of six propagating waves are expected to exist in the far field of the disturbance at large time. Since they have different group velocities, they separate from each other initially, which can be seen in figure 1. The fastest downstream-heading wave is  $k_4$  (with longest wavelength,  $C_{g,4} < 0$ ) and its interface image (note that  $k_4$  is a surface wave) is clearly seen on the right front side. Then wave  $k_8$  ( $C_{g,8} < 0$ ) is seen which is slower than wave  $k_4$  and appears downstream of the disturbance (still on the right-hand side of the disturbance at  $x = 0$ ). Other downstream waves in the plot are interfacial wave  $k_7$  ( $0 < C_{g,7} < U$ ), and interface image of surface waves  $k_1$  ( $0 < C_{g,1} < U$ ) and  $k_3$  ( $0 < C_{g,3} < U$ ). Note that waves  $k_7$ ,  $k_1$  and  $k_3$  are superimposed and occupy the region between  $-10 < k_0x < 0$  in figure 1 and are hardly distinguishable graphically. In front of the disturbance (on the left-hand side of the disturbance at  $x = 0$ ), only wave  $k_2$  ( $U < C_{g,2}$ ) appears and what is seen in the graph is the interface image of this wave. Surface waves follow a similar trend and thus are not shown here.

The numerical approach above is general for any value of  $\mathcal{R}$ . For numerical illustration in this paper, we have generally fixed  $\mathcal{R}=0.9$  which is lower than  $\mathcal{R}$  values in typical ocean environments ( $R \gtrsim 96$ ). In addition to accentuating some specific features for illustration, results for lower  $\mathcal{R}$  value may also be more relevant to comparisons with laboratory experiments (e.g.  $\mathcal{R}=0.85$  in Melville & Helfrich 1987 and  $\mathcal{R} \sim 0.5$  in Veletsos & Shivakumar 1993). In select cases, we present results with different values of  $\mathcal{R}$  (close to 1) (e.g.  $\mathcal{R}=0.95$  and  $\mathcal{R}=0.975$  in figure 4) to highlight quantitative differences among qualitatively similar results.

The ranges of other variables involved ( $\tau$ ,  $\mathcal{F}$  and  $h$ ) are nevertheless quite broad. Dimensionless depth  $h$  can vary from near zero (deep ocean) to close to unity (e.g. MacDonald & Hollister 1973). The Froude number  $\mathcal{F}$  can vary from zero (for slow speed or deep water) to unity and beyond particularly in shallower water (Alam & Mei 2008). For instance, in 10 m deep water, a speed of  $U \sim 10 \text{ m s}^{-1}$  corresponds to  $\mathcal{F} \sim 1$ . The dimensionless frequency  $\tau$  can go, theoretically, from zero (for slow translation) to very high values. For example, for a typical deep ocean wave of  $T = 8 \text{ s}$ , and current speed  $U \sim 10 \text{ m s}^{-1}$ ,  $\tau \sim 1.4$ .

## 5. Results and discussion

### 5.1. Resonance involving one oscillating frequency

We first consider the relatively simple cases involving one oscillation frequency for the disturbance. For class I resonance, as discussed in §3.1, the amplitude envelopes of the interacting waves can reach a steady state in the disturbance frame of reference after some time, with the amplitude of the resonance-generated wave given by a closed-form solution (3.3). We use this solution to cross-validate the direct simulation and the analysis.

Figure 2(a) shows the spatial growth of the resonant wave, after reaching a steady state, due to class I resonance obtained by the direct simulation. For this example, we use  $\mathcal{R}=0.90$  and  $h=0.005$  for the two-layer fluid (corresponding to a relatively deep lower layer compared with the upper layer), and  $\tau=0.4171$  and  $\mathcal{F}=0.004$  for the disturbance. With these parameters, we have a class I resonance formed by waves  $k_4$  and  $k_7$  and a resonant wave  $k_r = k_4 + k_7$ . For comparison, the analytic solution (3.3) for the growth of the resonant wave is also shown. It is seen that the direct simulation result compares very well with the analytic solution for the envelop of the amplitude of the resonant wave.

In terms of physical variables, the case in figure 2(a) corresponds to, for example, a disturbance moving with a speed of 17.3 knots while oscillating with a period of 13.5 s in a two-layer stratified sea of total depth 2 km with a thermocline located at 10 m below the sea surface. Waves  $k_4$ ,  $k_7$  and  $k_r$  are respectively the surface wave of  $\lambda_4 \approx 500 \text{ m}$  ( $T_4 \approx 18 \text{ s}$ ), interfacial wave of  $\lambda_7 \approx 90 \text{ m}$  ( $T_7 \approx 40 \text{ s}$ ) and resonant interfacial wave of  $\lambda_r \approx 76 \text{ m}$  ( $T_r \approx 34 \text{ s}$ ). If the source strength is such that the  $k_4$  wave has amplitude  $A_4=0.5 \text{ m}$  on the surface, and  $A_7=1 \text{ m}$  on the interface, the amplitude of the resonant interfacial wave ( $k_r$ ) grows up to  $A_r \approx 0.25 \text{ m}$  after a resonant interaction length of  $\sim 6\lambda_4$ , as seen in figure 2(a). The amplitude of the resonant wave is a quadratic function of the disturbance strength, and it quadruples if the disturbance strength doubles. Note that the frequencies of the interfacial waves in this example are much higher than the peak buoyancy frequency of an ocean thermocline and those of typical internal waves observed in the ocean (Munk 1980; Gargett & Holloway 1984). The high-frequency internal waves like these however

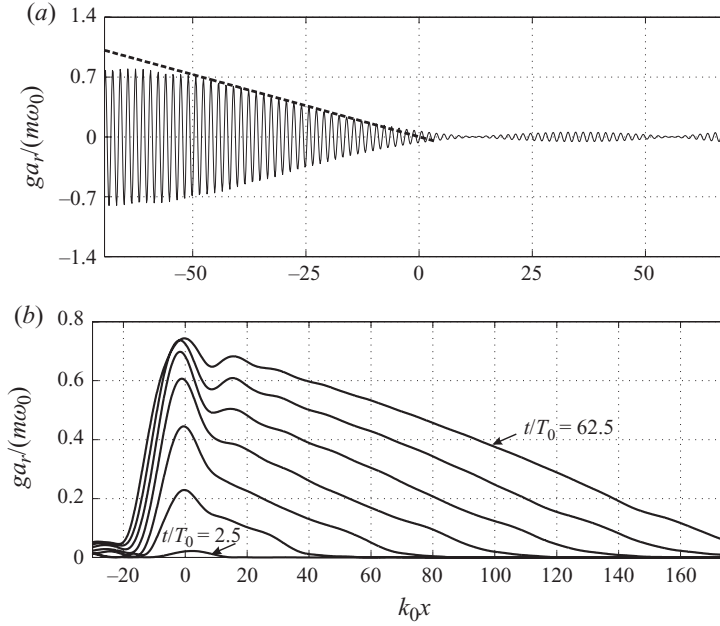


FIGURE 2. (a) Amplitude growth (after reaching a steady state) of the resonance-generated interfacial wave as a result of class I resonant interaction with waves  $k_4$  and  $k_7$  of a disturbance. Plotted are the direct simulation solution (—) and the perturbation solution (---) by (3.3). Physical parameters are  $\tau = 0.4171$ ,  $\mathcal{F} = 0.004$ ,  $\mathcal{R} = 0.90$  and  $h = 0.005$ ; numerical parameters are  $N = 4096$ ,  $N_t = 64$ ,  $M = 3$  and  $L = 80\lambda_4$ . (b) Time evolution of the amplitude of the resonant wave generated by group-b class II resonant interactions of the ambient head wave  $k_8$  and disturbance wave  $k_2$ . Curves plotted correspond respectively to  $t/T_0 = 2.5, 12.5, 22.5, 32.5, 42.5, 52.5$  and  $62.5$ . Physical parameters are  $\tau = 0.075$ ,  $\mathcal{R} = 0.9$ ,  $\mathcal{F} = 0.004$  and  $h = 0.12$ ; numerical parameters are  $N = 4096$ ,  $N_t = 64$ ,  $M = 3$  and  $L = 68\lambda_2$ .

have been reported in lakes and coastal waters (Garrett & Munk 1975; Boegman *et al.* 2003).

For class II resonance, group-a resonance behaves similarly to that of class I resonance. Unlike group-a resonance, group-b resonance envelopes do not reach steady state as we show in §3.3.2. Our direct numerical simulation confirms this distinctive feature of group-b (class II) resonance. Figure 2(b) shows the time evolution of the amplitude of the resonant wave associated with group-b resonance. For this numerical example, the ambient head-sea wave with  $k_a = k_8$  and the disturbance wave  $k_2$  generate a resonant free-wave ahead of the disturbance in the group-b resonance. Since the group speed of the resonant wave  $C_{g,r}$  is less than the speed of the disturbance  $U$ , this wave moves backward toward the disturbance (in the disturbance-fixed frame of reference) and eventually passes over it. As time grows, wave  $k_2$  marches forward and the length of the resonant interaction between  $k_2$  and  $k_8$  waves increases. Thus, as the result in figure 2(b) shows, the amplitude of the resonant wave near the disturbance increases with time. Since a cascade of such resonant interactions continues indefinitely both fore and aft of the disturbance, a steady state is not reached.

### 5.2. Generation of short waves by class II triad resonances

Class II-a resonance among the radiated and ambient waves can result in the generation of short wavelength resonant waves in the far-field upstream and/or

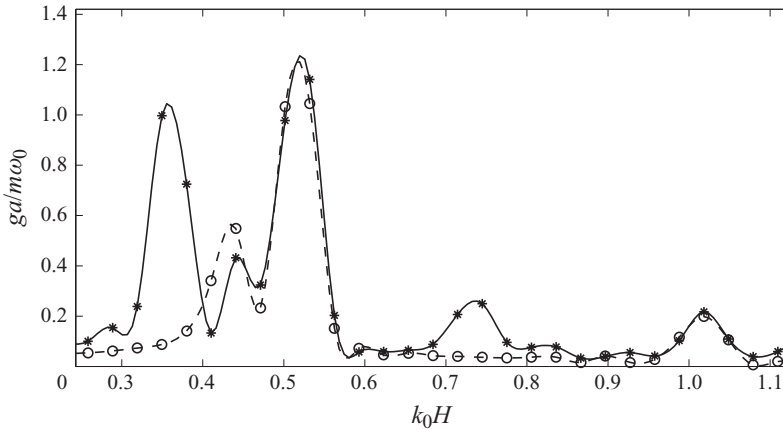


FIGURE 3. Nonlinear ambient wave amplitude spectrum (---,  $\circ$ ) and the total wavefield amplitude spectrum (—,  $*$ ) behind the body including both ambient waves and disturbance waves. Numerical parameters are  $N = 2048$ ,  $N_t = 64$ ,  $M = 3$  and  $L \approx 80 \lambda_8$ .

downstream of the disturbance. This occurs for two interacting waves of wavenumbers  $k'$  and  $k''$  forming a resonant triad with a wave of  $k_r = k' + k''$ .

Consider a scenario in which a moving disturbance responds to narrowband ambient waves in a range of motion frequencies within this band. In this case, short far-field resonant waves are generated as a result of triad interactions among the components of the radiated and ambient waves. For numerical illustration, we consider a case with  $\mathcal{R} = 0.9$  and  $h = 0.33$ . We assume that the ambient wavefield contains wave components  $k_{1,2,3,4}H = 0.44, 0.47, 0.50$  and  $0.53$  and amplitudes  $a_{1,2,3,4}/H = 0.007, 0.013, 0.013$  and  $0.007$ . We assume a moving disturbance in the lower fluid layer with  $\mathcal{F} = 0.032$  and  $z_0/H = 0.66$  whose response to the ambient waves contains frequencies corresponding to  $k_3$  and  $k_4$ , i.e.  $\tau_{3,4} = 0.073$  and  $0.069$  for the given  $\mathcal{F}$ . Figure 3 plots the amplitudes of the downstream waves over the wavenumber spectrum obtained using nonlinear direct computations for disturbance strengths  $m_3 = m_4 = 0.06\omega_0 H^2$ . As expected, the linear wake contains wave components at the range of  $0.3 < k_0 H < 0.6$ . Specifically, ambient wave spectrum has a primary (linear) peak at  $kH = 0.51$  and a smaller (second harmonic) peak near  $kH = 1.02$ . Due to disturbance-generated (linear) waves, another apparent peak appears at  $kH = 0.36$  which belongs to wave  $k_4$  of the disturbance. Other disturbance waves of interest are  $k_2 H = 0.53$ , which is at the same place as the primary peak of the ambient wave spectrum and  $k_8 H = 1.26$  of an interfacial wave.

Of particular interest is that the nonlinear wake in the presence of disturbance is significantly different in the shortwave part of the spectrum ( $k_0 H \approx 0.73$ ) where a significant peak is now formed due to triad-resonance interaction between ambient waves and disturbance waves. Specifically, ambient surface wave  $k_2$  and interfacial wave  $k_8$  form a triad resonance with a resonant wave  $k_r H = 0.73$  to create short waves near  $k_r H \approx 0.73$ . In the application, if a peak is observed around  $k_r H = 0.73$  by the above analysis (of surface wave data), we can deduce the presence of a object translating with  $\mathcal{F} = 0.032$ . This feature of triad resonance might be useful for interpreting remote sensing of short waves in the wake.

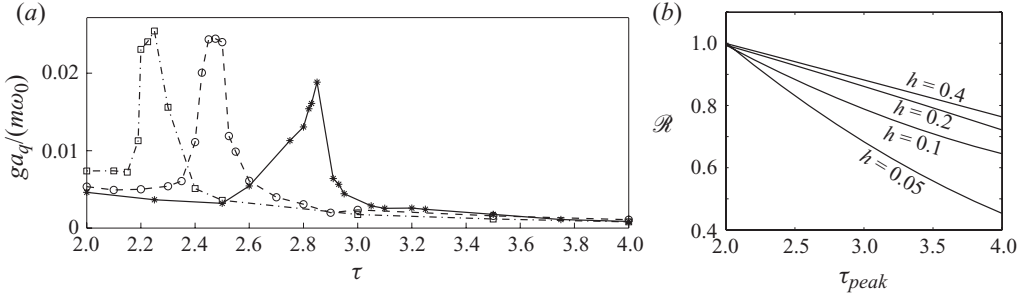


FIGURE 4. (a) The amplitude of  $k_q = k_4 - k_8$  wave in the wake of an oscillating and translating disturbance as a function of  $\tau$  for fixed  $\mathcal{F} = 0.6$ ,  $h = 0.33$ , and  $\mathcal{R} = 0.9$  (—, \*) , 0.95 (- - -,  $\circ$ ) and 0.975 (- · -,  $\square$ ). The simulation parameters are  $N = 2048$ ,  $N_t = 32$ ,  $M = 3$  and  $L = 150 \lambda_4$ . (b) Resonance condition for  $\mathcal{R}$  as a function of  $\tau_{peak}$  at different values of  $h$ .

### 5.3. Estimate of stratification properties from wave measurements

As illustrated above, class I and class II resonances occur at selective combinations of physical parameters resulting in distinctive wave signatures on the surface and interface. This provides the possibility of solving the inverse problem (see e.g. Avital & Miloh 1999) wherein ocean stratification properties or current speed can be estimated based on measurements of surface and/or interface resonant waves.

As an illustration, we consider a scenario in which we use the measurement of a class I resonant surface wave to estimate the fluid density ratio  $\mathcal{R}$ . For this purpose, we assume a moving disturbance capable of oscillating in a range of frequencies (by, say, appropriate tuning of mass or buoyancy properties in the presence of multi-chromatic ambient waves). For specificity, we assume that the amplitude of  $k_q \equiv k_4 - k_8$  wave in the wake behind the disturbance is measured. Note that  $k_4$  and  $k_8$  are the only two disturbance waves that have negative group velocity with respect to the translation direction of the disturbance, and hence they can easily be identified. For given  $\tau$ ,  $\mathcal{F}$  and  $h$ , in theory, the second-order resonant interaction between  $k_4$  and  $k_8$  waves occurs at a specific value of  $\mathcal{R}$ . Thus, the determination of the critical  $\tau$  value at which  $k_q$  wave becomes resonant gives a unique estimate of  $\mathcal{R}$ .

Figure 4 shows a numerical example for which  $h = 0.33$  and  $\mathcal{F} = 0.6$  are assumed to be known. The disturbance goes through a range of frequencies in its oscillating motion corresponding to  $2 < \tau < 4$ . For each oscillating frequency, the amplitude of wave  $k_q$  is measured, which is shown in figure 4(a). It is seen that the amplitude reaches an extremum at a specific frequency  $\tau_{peak}$ , corresponding to class I resonance. From the resonance condition,  $\mathcal{R}$  can be determined from  $\tau_{peak}$  given  $h$  and  $\mathcal{F}$ , as illustrated in figure 4(b). Because of the nature of class I triad resonance, the amplitude of the resonant wave drops sharply around  $\tau_{peak}$  (figure 4a) so that the estimation of  $\mathcal{R}$  (given  $h$  and  $\mathcal{F}$ ) is much more precise relative to, say, those based on measurements of linear wavefield. In figure 4(a), we present the results corresponding to  $\mathcal{R} = 0.9$ , 0.95 and 0.975. The results with different values of  $\mathcal{R}$  show a similar qualitative behaviour with slightly higher resonant-wave amplitude and lower  $\tau_{peak}$  for weaker stratification.

Variations to this scheme, for example, estimating  $h$  given  $\mathcal{R}$  and  $\mathcal{F}$ , or  $\mathcal{F}$  given  $\mathcal{R}$  and  $h$ , obtain in a similar way.

#### 5.4. Multiple resonances and their interactions

If a moving body responds at multiple frequencies to broadband ambient waves, multiple-resonant (and near-resonant) interactions among the ambient waves and the disturbance waves may occur at second (discussed so far) and higher orders. The interesting question is whether we can characterize the far-field wake wave spectrum resulting from (cascades of) such multiple resonances.

The nonlinear numerical method we develop is capable of accounting for these interactions up to an arbitrary high order. As a final illustration, we consider this scenario for a special case, say, with  $\mathcal{F} = 0.032$ ,  $z_0/H = 0.1$ ,  $\mathcal{R} = 0.9$  and  $h = 0.2$ . For definiteness, we assume that the disturbance oscillates at three distinct frequencies corresponding to  $\tau^{(1,2,3)} = 0.24, 0.49$  and  $0.58$ . For these parameters, two second-order triad resonances occur initially leading to new resonant waves with wavenumbers  $k_{r_1}H = k_7^{(1)}H - k_4^{(2)}H = 4.9$  and  $k_{r_2}H = k_8^{(2)}H - k_8^{(3)}H = -1.6$ , where  $k_j^{(i)}$  denotes the  $j$ th wave associated with disturbance oscillation at frequency  $\tau_i$ . In this case,  $k_{r_1}$  and  $k_{r_2}$  refer to surface-mode waves with encounter frequencies  $\omega_{r_1}^{en}/\omega_0 = 1.042$  and  $\omega_{r_1}^{en}/\omega_0 = -0.847$ . These resonant waves will further participate in a number of near-resonance interactions with other wake waves. The introduction of the ambient wave components introduces additional (near) resonances (and resulting complexities), which, for simplicity, we exclude in the numerical simulation.

Figure 5 compares the far-field wave amplitudes over a broad range of  $\omega$  behind the disturbance for the disturbance in a homogeneous fluid ( $\mathcal{R} = 1$ ) and a two-layer fluid ( $\mathcal{R} = 0.9$ ). The spectra are computed at two locations with  $x_1/H = 16$  (figure 5*a, c*) and  $x_2/H = 37$  (figure 5*b, d*) from the disturbance. In terms of physical parameters and in a sea of the total depth of  $H = 100$  m and the thermocline depth of  $h_u = 20$  m, this case corresponds to a disturbance with the periods of oscillation of  $T^{(1,2,3)} = 15, 7.3$  and  $6$  s, and amplitudes are calculated at the physical distances of  $1.6$  and  $3.7$  km behind the disturbance

Referring to figure 5, due to nonlinear resonant interactions energy transfers among interacting wave modes as they propagate downstream. In the presence of multiple-resonant and near-resonant interactions, the energy transfer among various interacting wave modes is enhanced, leading to a broadband spectrum, as shown in figure 5(*d*). As the interaction length increases, the amplitude spectrum is seen to spread over a band of frequencies wherein the peak associated with the dominant linear encounter frequency ( $\omega_{en} = 5.48$ ) cannot be distinguished from the background resonant and free waves.

## 6. Concluding remarks

The problem of resonant (nonlinear) wave generation in the wake of an oscillating and translating disturbance in a two-layer fluid is considered. It is shown that disturbance wake waves, upon nonlinear interaction among themselves and/or with ambient waves that caused the motion, may generate resonant-free waves at the second order as part of a triad of wave components. The resonant wave can form in the upstream or downstream of the disturbance and may propagate towards or away from the disturbance. Evolution of the resonant wave is studied analytically using perturbation theory.

For the more general case of multiple ambient and radiated wave components that may be resonantly interacting, an HOS method is developed that can take into account a large number of wave components and arbitrary high order of nonlinear interactions. As an illustration of the effect of multiple resonances, it is shown that

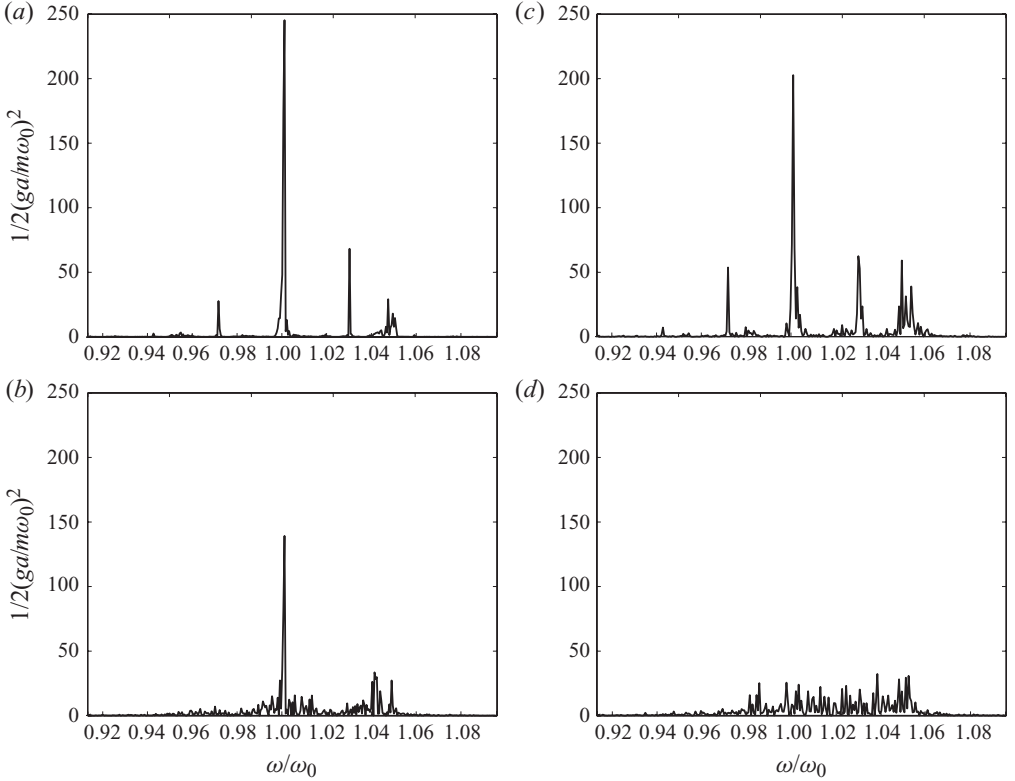


FIGURE 5. Amplitude spectrum of surface waves behind the disturbance in a homogeneous fluid of  $\mathcal{R} = 1.0$  (*a, b*) and a two-layer stratified fluid of  $\mathcal{R} = 0.9$  (*c, d*). Plotted are the amplitude spectrum of wave elevations respectively at  $x_1/H = 16$  (*a, c*) and  $x_2/H = 37$  (*b, d*) behind the disturbance. Parameters are  $\mathcal{F} = 0.032$ ,  $h = 4$  and the disturbance oscillates with three frequencies:  $\tau^{(1)} = 0.24$ ,  $\tau^{(2)} = 0.49$  and  $\tau^{(3)} = 0.58$ .

nonlinear interaction between a narrowband ambient wave and the radiated waves from a moving and oscillating disturbance can result in an isolated high-frequency peak in the downstream spectrum, which may facilitate its quantification by remote sensing. We also show that the sensitivity of resonance offers a useful scheme for precise estimation of ocean physical properties such as density stratification.

When the disturbance undergoes an oscillation with multiple frequencies, our numerical simulations show that the resultant cascades of multiple-resonant interactions lead to the spread of wave energy in the far-field wake into a broad frequency band. This phenomenon is not obtained in a homogeneous fluid or in the absence of nonlinear resonance.

We note that the similar resonant phenomenon should also be obtained in three dimensions, but with more complex features. Unlike in two dimensions, the wavenumber of the disturbance waves is now a function of the angle of the ray (relative to forward direction), and furthermore their amplitudes must now necessarily decay with distance from the disturbance. Resonant interactions are expected to occur along specific rays angles determined by three-dimensional resonance conditions, and new resonant waves are generated in the neighbourhood of these resonance rays as a consequence (see, e.g. Zhu *et al.* 2008, for this problem in the homogeneous

fluid case). Generalization of this work to three dimensions could therefore be of theoretical and practical interest.

We are not aware of direct field or laboratory observations of the effects we describe. We believe that the present study could provide a predictive framework to evaluate the possibility of such measurements.

## REFERENCES

- AKYLAS, T. R. 1984 On the excitation of nonlinear water waves by a moving pressure distribution oscillating at resonant frequency. *Phys. Fluids* **27** (12), 2803–2807.
- AKYLAS, T. R. 1987 Unsteady and nonlinear effects near the cusp lines of the Kelvin ship-wave pattern. *J. Fluid Mech.* **175**, 333–342.
- ALAM, M.-R. 2008 Interaction of waves in a two-layer density stratified fluid. PhD thesis, Massachusetts Institute of Technology, Cambridge, MA.
- ALAM, M.-R., LIU, Y. & YUE, D. K. P. 2009a Waves due to an oscillating and translating disturbance in a two-layer density-stratified fluid. *J. Engng Maths* **65** (2), 179–200.
- ALAM, M.-R., LIU, Y. & YUE, D. K. P. 2009b Bragg resonance of waves in a two-layer fluid propagating over bottom ripples. Part I. Perturbation analysis. Part II. Numerical simulation. *J. Fluid Mech.* **624**, 191–253.
- ALAM, M.-R. & MEI, C. C. 2008 Ships advancing near the critical speed in a shallow channel with a randomly uneven bed. *J. Fluid Mech.* **616**, 397.
- AVITAL, E. & MILOH, T. 1994 On the determination of density profiles in stratified seas from kinematical patterns of ship-induced internal waves. *J. Ship Res.* **38** (4), 308–318.
- AVITAL, E. & MILOH, T. 1999 On an inverse problem of ship-induced internal waves. *Ocean Engng* **26** (2), 99–110.
- BALL, F. 1964 Energy transfer between external and internal gravity waves. *J. Fluid Mech.* **19**, 465–478.
- BOEGMAN, L., IMBERGER, J., IVEY, G. N. & ANTENUCCI, J. P. 2003 High-frequency internal waves in large stratified lakes. *Limnol. Oceanogr.* **48** (2), 895–919.
- CRAIK, A. D. D. 1988 *Wave Interactions and Fluid Flows*. Cambridge University Press.
- DAGAN, G. & MILOH, T. 1982 Free-surface flow past oscillating singularities at resonant-frequency. *J. Fluid Mech.* **120**, 139–154.
- DEBNATH, L. 1994 *Nonlinear Water Waves*. Academic.
- DOMMERMUTH, D. G. & YUE, D. K. P. 1987 A higher-order spectral method for the study of nonlinear gravity waves. *J. Fluid Mech.* **184**, 267–288.
- D'YACHENKO, A. I. & ZAKHAROV, V. E. 1994 Is free-surface hydrodynamics an integrable system? *Phys. Lett. A* **190** (2), 144–148.
- FALTINSEN, O. M. 1993 *Sea Loads on Ships and Offshore Structures*. Cambridge University Press.
- GARGETT, A. E. & HOLLOWAY, G. 1984 Dissipation and diffusion by internal wave breaking. *J. Mar. Res.* **42** (1), 15–27.
- GARRETT, C. & MUNK, W. 1975 Space-time scales of internal waves: a progress report. *J. Geophys. Res.* **80** (3), 291–297.
- GARRETT, C. & MUNK, W. 1979 Internal waves in the ocean. *Annu. Rev. Fluid Mech.* **11** (1), 339–369.
- HAMMACK, J. L. & HENDERSON, D. M. 1993 Resonant interactions among surface water waves. *Annu. Rev. Fluid Mech.* **25** (1), 55–97.
- HILL, D. F. & FODA, M. A. 1996 Subharmonic resonance of short internal standing waves by progressive surface waves. *J. Fluid Mech.* **321**, 217–233.
- KUNZE, E., ROSENFELD, L. K., CARTER, G. S. & GREGG, M. C. 2002 Internal waves in Monterey submarine canyon. *J. Phys. Oceanogr.* **32**, 1890–1913.
- LAMB, H. 1932 *Hydrodynamics*. Dover.
- LIU, Y. & YUE, D. K. P. 1993 On the solution near the critical frequency for an oscillating and translating body in or near a free surface. *J. Fluid Mech.* **254**, 251–266.
- MACDONALD, K. C. & HOLLISTER, C. D. 1973 Near-bottom thermocline in the Samoan Passage, west equatorial Pacific. *Nature* **243**, 461–462.
- MELVILLE, W. K. & HELFRICH, K. R. 1987 Transcritical two-layer flow over topography. *J. Fluid Mech.* **178**, 31–52.

- MUNK, W. H. 1980 Internal wave spectra at the buoyant and inertial frequencies. *J. Phys. Oceanogr.* **10** (11), 1718–1728.
- NEWMAN, J. N. 1971 Third order interactions in the Kelvin ship wave systems. *J. Ship Res.* **15**, 1–10.
- STAQUET, C. & SOMMERIA, J. 2002 Internal gravity waves: from instabilities to turbulence. *Annu. Rev. Fluid Mech.* **34** (1), 559–593.
- VELETSOS, A. S. & SHIVAKUMAR, P. 1993 Sloshing response of layered liquids in rigid tanks. *Tech. Rep.* BNL-52378, Brookhaven National Lab., Upton, NY.
- WEN, F. 1995 Resonant generation of internal waves on the soft sea bed by a surface water wave. *Phys. Fluids* **7** (8), 1915–1922.
- WREN, G. G. & MAY, D. 1997 Detection of submerged vessels using remote sensing techniques. *Aust. Def. Force J.* **127**, 9–15.
- ZHU, Q., LIU, Y. & YUE, D. K. P. 2008 Resonant interactions between Kelvin ship waves and ambient waves. *J. Fluid Mech.* **597**, 171–197.